



Soil selenium transformation across different parent materials in Pothwar uplands of Pakistan

Muhammad Imran¹ · Mohammad Saleem Akhtar² · Ayaz Mehmood³ · Shah Rukh⁴ · Ahmad Khan² · Chen Zhikun⁵ · Ghulam Mujtaba²

Received: 18 February 2020 / Accepted: 6 October 2020 / Published online: 15 October 2020
© Saudi Society for Geosciences 2020

Abstract

Selenium (Se) is an essential trace element for humans but non-essential for plants. Selenium bioavailability depends on selenium forms in soil. Selenium contents may vary with the source of parent material, and pedogenesis controls its vertical distribution. The objectives of this study were to determine the variation in Se fractions with parent material and pedogenesis in Pothwar uplands of Pakistan. Triplicate soil profiles at different development stages from selected parent materials (sandstone, alluvium, loess, and shale) were sampled at different genetic horizons level. The soils were characterized for pH, dissolved organic carbon, total organic carbon, dithionite extractable amorphous iron, and cation exchange capacity. Soil selenium was fractionated into ion-exchangeable, metal oxides, organic, humic, sulfide, and residual selenium. Selenium in the soil extract was measured using HVG-AAS after centrifuge and passing through a 0.45- μm cellulose free filter. The distribution of total selenium content and selenium fractions varied with the type of parent material and soil genesis. Total selenium contents differed significantly across the different parent material. The highest total selenium was in shale followed by loess, alluvium, and sandstone, respectively. Exchangeable ion, metal oxides, and organic matter selenium were more in loess or the same level as of shale. Evaluation of the distribution of selenium fractions enabled us to estimate the occurrence of potential selenium deficiency and toxicity to humans and animals based on the parent materials and pedogenesis.

Keywords Selenium distribution · Soil genesis · Weathering stages · Parent materials · Pakistan

Introduction

Selenium is an essential trace element for animals, and intermediate between metals and non-metals (Kurokawa and Berry

2013). It plays important biological functions, and its deficiency causes serious health problems, while in higher concentrations it becomes toxic (Yatoo et al. 2013; Natasha et al. 2018). Distribution of total selenium content in soils is controlled by the composition of parent materials, and the soil-forming processes (Xing et al. 2015; Imran et al. 2016). Selenium-rich soils are formed from shale parent material because of their high total selenium content (Parnell et al. 2018). Soil genesis controls the release of selenium through the weathering of minerals, redistribution, and transformation. The soils developed from rocks with high selenium contents under rainfall < 500 mm contain potentially toxic levels of selenium. However, the soils originating from the same parent material in humid regions had high selenium contents that were bound to iron oxides. Besides the role of climate, the transformation, soils, developed from the parent material with lower selenium content are deficient in selenium. (Lopes et al. 2017).

Selenium transformation in the natural soil environment, regarding the effect of parent material and weathering on the distribution of selenium fractions in alluvium, loess, sandstone, and shale-derived soils, is very little. The relationship

Responsible Editor: Stefan Grab

✉ Muhammad Imran
changwani_baloch2005@yahoo.com; imranm@gudgk.edu.pk

¹ Department of Soil and Environmental Sciences, Ghazi University, Dera Ghazi Khan, Pakistan

² Institute of Soil Science, PMAS-Arid Agriculture University Rawalpindi, Rawalpindi, Pakistan

³ Department of Soil and Climate Sciences, University of Haripur, Haripur, Pakistan

⁴ National Centre of Excellence in Geology, University of Peshawar, Peshawar, Pakistan

⁵ Key Laboratory of Soil Resource & Biotech Application, Xi'an Botanical Garden of Shaanxi (Institute of Botany Shaanxi Province), Shaanxi Academy of Sciences, Xi'an 710061, China

between selenium fractions following pedogenesis and parent material in calcareous soil systems of arid and semiarid regions needs to be assessed. In this study, it was hypothesized that selenium contents differ across the soil parent materials and weathering which affects the distribution of selenium fractions within a parent material. The current study quantifies the distribution of selenium and its fractions in soils of each parent material with the main objective to predict the effect of weathering stage on selenium distribution.

Materials and methods

Soil description and sampling

The soil sampling from the study area comprising of all four parent materials (i.e., alluvium, loess, sandstone, and shale) are presented in Fig. 1. The soils of residuum shale and sandstone are of Miocene epoch and loess of Pleistocene epoch; alluvium is of the Holocene and Pleistocene epochs. The soils at their different development stages were selected from various parent materials that are loess, alluvium, sandstone, and shale. In the study area, loess is the dominant type of parent material and deposited during the Pleistocene period. Whereas, the present land morphology is created by sub-Recent erosion and deposition cycle. In the loess parent material, Chakwal soil series from level plains, Rawalpindi soil series from nearly level to gently sloping area, and Rajar soil series from gullied land were selected. Alluvium occurred as narrow strips along with the courses of the Indus river

tributaries. Soil development in alluvial sediments depends upon the chronosequence. The Gujranwala soil series from the late Pleistocene period, Argan soil series formed in Sub-recent alluvium, and Shahdara soil series from Recent alluvium were selected. The Siwalik formation of the Pliocene period comprises sandstone, whereas the Murree formation of the Miocene period has shale parent material, with both their formations, host residual soils where relief played an important role in the soil genesis. The Kahuta soil in sandstone is developed on a leveled area with a sub-humid, sub-tropical, continental climate, while the Balkasar soil is developed in calcareous sandstone in low lying areas, and the Qazian soil developed in the foothills. The Murree formation consists of red and purple tertiary shale. The Murree soil is developed at level areas and is decalcified due to effective rainfall. The Tirnul soil series is moderately deep and well-drained. The Ghoragali soil series least weathered consists of moderately deep and drained, calcareous without the Cambic B horizon. The soil occupies mountain slopes and alpine forests developed in the residuum, therefore, least differentiated. The three soil profiles for each series were dug (Table 1) and described. The soil samples from each genetic horizon were collected, air-dried, and passed through a 2-mm sieve before analysis.

Soil characterization

All the soil samples were characterized for texture, soil pH, oxidation–reduction potential, calcium carbonate content, total and dissolved organic carbon, dithionite extractable iron, oxalate extractable iron, and cation exchange capacity (CEC).

Fig. 1 Study area indicating sampling points of alluvium, loess, sandstone and shale parent materials

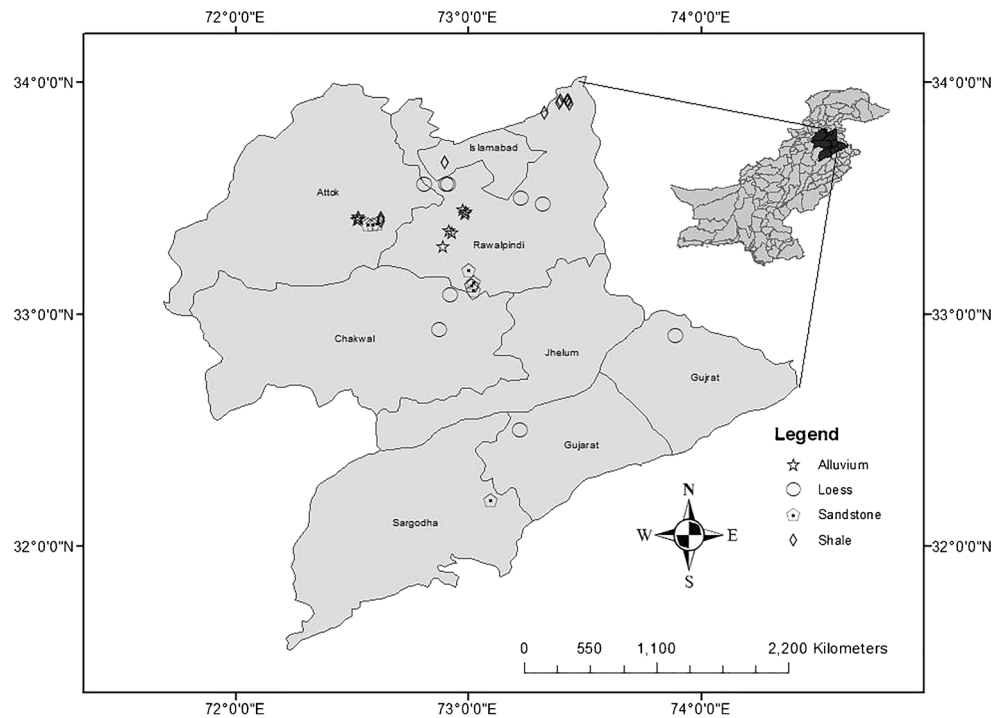


Table 1 The selected soil series (USDA classification)

Parent material	Least weathered soil	Moderately weathered soil	Weathered soil
Loess	Rajar (Typic Ustorthents)	Rawalpindi (Udic Haplustepts)	Chakwal (Typic Haplustalfs)
Alluvium	Shahdra (Typic Ustifluents)	Argan (Fluventic Haplustepts)	Gujranwala (Typic Haplustalfs)
Sandstone residuum	Qazian (Lithic Ustipsamments)	Balkasar (Typic Haplustalfs)	Kahuta (Udic Haplustalfs)
Shale residuum	Ghoragali (Typic Udorthents)	Tirnul (Typic Haplustepts)	Murree (Typic Hapludolls)

Saturated soil paste was used for measuring soil pH (McLean 1982) after 30-min equilibrium time. Redox potential was determined in 1:1 soil to water suspension by a combined electrode before calibrating with ZoBell's solution. Calcium carbonate was quantified by the acetic acid (CH₃COOH) consumption method (Loeppert et al. 1984). Soil total organic carbon was determined in each sample by titrating against ferrous ammonium sulfate (Fe(NH₄)₂(SO₄)₂) solution, after wet digestion in potassium dichromate (K₂Cr₂O₇) and concentrated sulfuric acid (Walkley 1947). Dissolved organic carbon (DOC) was measured after extraction with potassium sulfate, and digesting with K₂Cr₂O₇ and concentrated H₂SO₄. The ferrous ammonium sulfate was used to measure excessive potassium dichromate (Nelson and Sommers 1982).

Total iron contents were extracted by sodium citrate (C₆H₅Na₃O₄.2H₂O), and sodium bicarbonate (NaHCO₃) buffer in the presence of sodium dithionite (Na₂S₂O₄) (Mehra and Jackson 1960). Amorphous iron was extracted in acidified ammonium oxalate monohydrate ((NH₄)₂C₂O₄.H₂O) solution (Jackson et al. 1986). The iron content in extracts was measured using the atomic absorption spectrophotometer. The cation exchange capacity of the soils was measured by extracting the sodium from exchange sites with ammonium following the measurement of sodium concentration extract by a Flame Photometer.

Sequential extraction of soil selenium

Total soil selenium was fractionated into six fractions viz. ion exchange and carbonate bound selenium, manganese-iron oxide bound selenium, organic matter bound selenium, humic compounds bound selenium, sulfide bound selenium, and recalcitrant selenium in residues. The sequential extraction scheme of Hagrova et al. (2005) was adopted (Table 2).

Statistical analysis

The variability in soil characteristics, total selenium, and Se fractions was analyzed using multivariate analysis. Parent materials were class variables and "soil" nested within the parent materials, while the measurements at different genetic horizons were multiple dependent variables. The multivariate

analysis (MANOVA) was implemented using Proc General Linear Model in SAS version 9.4. (SAS Institute Inc. 2002)

Result

Soil characteristics

In most of the soils, the CaCO₃, TOC, DOC, pH, Eh, CEC, and extractable Fe were controlled by the degree of weathering processes in each landscape position. Overall, the soils were non-calcareous to strongly calcareous, where the CaCO₃ content varied with the soil development. Calcium carbonate distribution in the soils at different weathering stages conformed to previously reported ranges (Amin and Ikram 2007). The subsurface accumulation of CaCO₃, due to leaching from the soil surface, causes dilution of other mineral phases and ionic species (Mayorga et al. 2019). The results are presented on a calcium carbonate free basis to remove the dilution effect (Table 2).

Total organic carbon content, though limited to the surface horizons, was high in soils of the shale parent material followed by the sandstone, loess, and alluvium. Total organic carbon varied with depth in all parent materials when averaged over the soils. The difference in parent material was significant at each depth in profile ($p \geq 0.01$). The distribution of TOC in soils at the three different landscape positions in each parent material differed statistically. Mean dissolved organic carbon was statistically similar when averaged over the soil type. The depth levels \times parent material interaction for dissolved organic carbon was non-significant ($F = 7.71$, $df = 12$, $p \geq 0.0001$), implying that change in DOC with depth was uniform in all parent material when averaged over the soils types.

Soil pH ranged from 6.5 to 8.2 and was significantly high in alluvium and loess, followed by the sandstone and shale. The soil pH at the three weathering stages in each parent material differed statistically as the hypothesis of depth level \times soil (pm) effect was accepted ($F = 1.20$, $df = 32$, $p \geq 0.26$). On the whole, the soils relatively at an older stage of development had relatively lower pH than the younger and moderately developed soils. Soil redox potential (Eh) ranged from 218 to 400 mV, and the mode value of the dataset was 247 mV. The mean Eh (mV) was significantly high ($F = 165$, $df = 3$, $p \geq$

0.0001) in shale and loess than sandstone and alluvium (Table 3).

Shale-derived soils had the maximum cation exchange capacity, and the sandstone soils had the lowest values (Appendix Table 5) which correlate with the clay contents. The siliceous material sandstone and light texture alluvium contain dominantly quartz, while the shale containing argillaceous clays (smectite and vermiculite) creates the difference in CEC. Mafic character leads to the increased CEC in any of the parent material (Santos et al. 2016). Cation exchange capacity increased with advanced weathering in this limited soil formation ranging from Entisols to Alfisols.

Extractable iron oxides were significantly more in the shale soils, and subsequently the alluvium, loess, and sandstone. Table 3 presents mean dithionite extractable iron oxides content in soils of four different parent materials, where the mean values ($n = 45$) are on calcium carbonate free basis. High extractable iron content in the shale soils is related to lithogenic iron contents (Mehmood et al. 2018; Fan et al. 2018). The depth levels \times parent material interaction for the extractable iron oxides content was accepted ($F = 1.33$, $df = 12$, $p \geq 0.23$), implying that the means soil iron oxides content at various depths remained unchanged when averaged over the soils.

Total selenium

The lowest total selenium $270 \mu\text{g kg}^{-1}$ was in sandstone, and the highest $7050 \mu\text{g kg}^{-1}$ was in the shale soils, while the parent material was the main source of variability. The soils developed from the shale parent material had the highest selenium contents ranging from 740 to $7050 \mu\text{g kg}^{-1}$ with the highest mean selenium ($n = 45$), whereas the loess, alluvium, and sandstone were statistically similar ($F = 11.37$, $df = 12$, $p \geq 0.0001$). The hypothesis of depth levels \times parent material interaction was rejected and the interaction was associated with high total selenium content at the surface contributed by the organic selenium (Fig. 2). Nevertheless, the difference in mean ($n = 15$) for parent material remained statistically significant throughout the depth. The soil genesis in each parent material changed the total selenium distribution differently. The difference in mean ($n = 3$) total selenium at different depths varied with soil genesis as depth levels \times soil (pm) interaction was rejected ($F = 6.53$, $df = 32$, $p \geq 0.0001$). In the shale and loess soil, the total selenium decreased with the soil depth in relatively more developed soils. This might be due to high organic matter at the soil surface (Table 4). The high organic matter at the surface of the Murree soils may have resulted in high total selenium. Pearson coefficient correlation (r) between organic carbon and total selenium content was 0.48.

The Hapludoll on the shale had a mollic epipedon resulting in higher mean Se values; similarly, the Ghoragalli soil had

very high organic carbon at the surface. Although less pronounced in the loess Alfisols, greater selenium at the surface of Chakwal soil series was observed and was associated with the accumulation of organic matter. Later, we demonstrated that the greater total selenium was due to greater organic selenium.

Soil selenium fractions

The total soil selenium partitioned into exchangeable, metal oxides bound, organic matter bound, humic acid bound, sulfide bound, and residual selenium and determined through the sequential extraction scheme of Hagrova et al. (2005) is present here. The distribution of these forms changed in the profile differently across the parent materials and soil genesis.

Water soluble and exchangeable selenium

The selenium fraction extracted with ammonium acetate, known as water-soluble and exchangeable selenium, varied between 18 and $170 \mu\text{g kg}^{-1}$ soil in the dataset. The water-soluble and exchangeable selenium had a positive correlation with cation exchange capacity ($r = 0.44$), organic selenium ($r = 0.36$), humic selenium ($r = 0.35$), and the relation with extractable, crystalline, and amorphous iron was though significant but had very low correlation coefficient.

The hypothesis of depth levels \times parent material interaction was accepted ($F = 1.48$, $df = 12$, $p \geq 0.16$) for water-soluble and exchangeable selenium, implying that the selenium fraction concentration at different depths varied and non-significantly with the source of parent material (Table 4). The highly weathered soils derived from the loess and shale had high water-soluble and exchangeable selenium concentration, especially in the surface horizons. The Shahdara soils occurred along with the river courses contaminated by city effluents and had high exchangeable selenium among the alluvial soils, although it was the least homogenized (Fig. 3). The hypothesis of depth levels \times soil(pm) interaction could not be rejected ($F = 1.27$, $df = 32$, $p \geq 0.20$), implying that the overall water-soluble and exchangeable selenium contents remained statistically similar throughout the profiles depth with weathering stage indicated by the soil type in each parent material. Water-soluble and exchangeable selenium was strongly related to the phosphate buffer extractable selenium with the Pearson coefficient ($r = 0.98$).

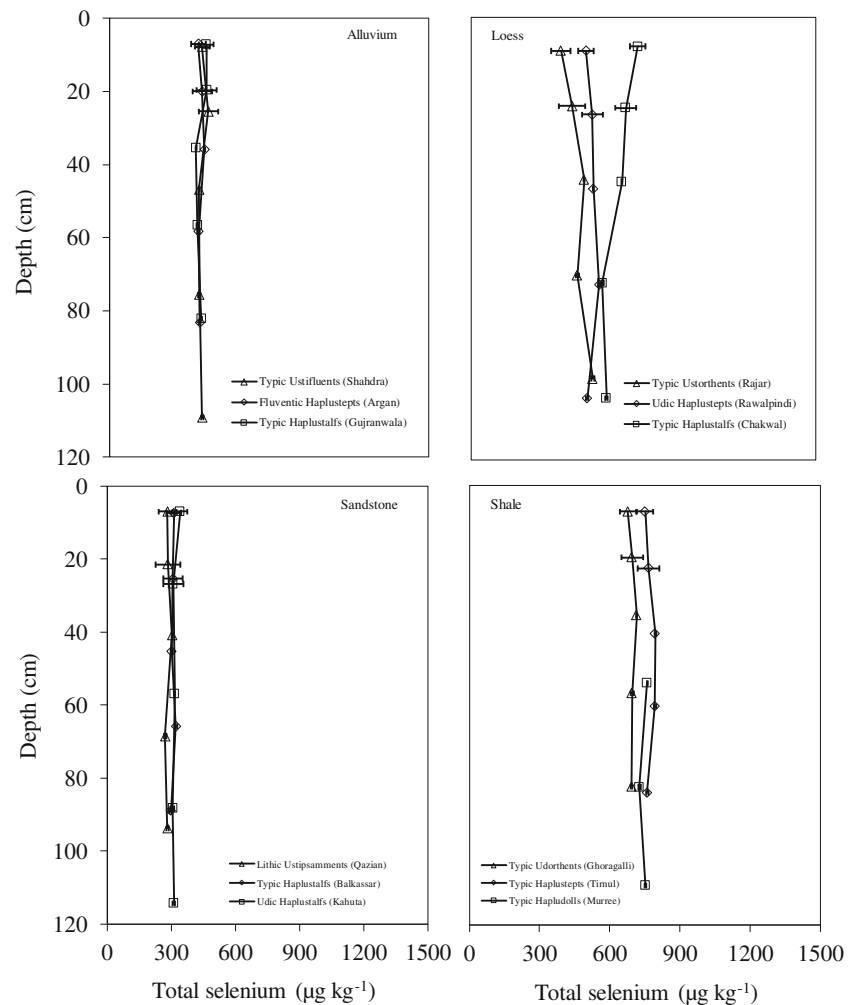
Metal oxide selenium

Iron and manganese oxides bound selenium, extracted during the dissolution of amorphous form of soil oxides by hydroxyl ammonium chloride treatment known as “metal oxides selenium,” ranged from 4 to $322 \mu\text{g kg}^{-1}$ soil with mean value $37 \mu\text{g kg}^{-1}$ soil. Metal oxide selenium concentration was the

Table 3 Soil pH, Eh, dissolved organic carbon, and clay contents for each soil in various parent materials

	Horizon				Loess			Sandstone				Shale		
	Alluvium		Argan		Gujranwala	Rejar	Rawalpindi	Chakwal	Qazian	Balkassar	Kahuta	Ghoragali	Timul	Murree
pH	Ap/A	7.60 _(0.20)	7.66 _(0.19)	7.27 _(0.15)	7.96 _(0.24)	7.08 _(0.20)	7.52 _(0.17)	7.54 _(0.23)	7.63 _(0.19)	6.88 _(0.20)	7.18 _(0.18)	7.59 _(0.22)	6.54 _(0.20)	
	BA	7.73 _(0.27)	7.69 _(0.25)	7.27 _(0.30)	8.11 _(0.33)	7.42 _(0.23)	7.50 _(0.27)	7.62 _(0.25)	7.62 _(0.25)	6.94 _(0.27)	7.46 _(0.21)	7.41 _(0.24)	6.29 _(0.23)	
	Bw/Bt	7.82 _(0.27)	7.73 _(0.27)	7.33 _(0.22)	8.14 _(0.33)	7.30 _(0.25)	7.49 _(0.23)	7.49 _(0.23)	7.52 _(0.26)	7.58 _(0.25)	7.04 _(0.27)	7.53 _(0.24)	6.38 _(0.20)	
	Bt/Btk	7.82 _(0.11)	7.67 _(0.10)	7.31 _(0.11)	8.18 _(0.13)	7.58 _(0.14)	7.37 _(0.21)	7.37 _(0.21)	7.68 _(0.14)	7.74 _(0.13)	7.12 _(0.11)	7.52 _(0.20)	7.80 _(0.18)	7.48 _(0.16)
	C1	7.85 _(0.11)	7.70 _(0.11)	7.47 _(0.11)	8.06 _(0.13)	7.70 _(0.13)	7.55 _(0.15)	7.55 _(0.15)	7.69 _(0.13)	7.80 _(0.11)	7.22 _(0.11)	7.56 _(0.20)	7.87 _(0.13)	7.44 _(0.20)
Eh (mV)	Ap/A	246 ₍₂₎	246 ₍₄₎	233 ₍₅₎	241 ₍₄₎	289 ₍₅₎	254 ₍₄₎	236.8 ₍₃₎	227 ₍₅₎	266 ₍₄₎	244 ₍₃₎	246 ₍₂₎	354 ₍₄₎	
	BA	242 ₍₃₎	245 ₍₅₎	228 ₍₆₎	241 ₍₅₎	267 ₍₅₎	262 ₍₄₎	232.3 ₍₃₎	223 ₍₆₎	263 ₍₃₎	267 ₍₃₎	244 ₍₂₎	398 ₍₅₎	
	Bw/Bt	248 ₍₂₎	241 ₍₃₎	248 ₍₇₎	240 ₍₃₎	277 ₍₆₎	265 ₍₄₎	243.4 ₍₅₎	233 ₍₅₎	270 ₍₄₎	262 ₍₂₎	235 ₍₃₎	393 ₍₄₎	
	BC1	247 ₍₅₎	253 ₍₄₎	246 ₍₅₎	234 ₍₄₎	281 ₍₂₎	264 ₍₃₎	242 ₍₃₎	235 ₍₄₎	261 ₍₄₎	251 ₍₂₎	232 ₍₂₎	352 ₍₅₎	
	BC2	249 ₍₄₎	267 ₍₄₎	246 ₍₅₎	242 ₍₅₎	286 ₍₃₎	265 ₍₃₎	233 ₍₅₎	233 ₍₅₎	257 ₍₃₎	252 ₍₄₎	228 ₍₃₎	346 ₍₅₎	
DOC (mg kg ⁻¹)	Ap/A	56.95 ₍₁₂₎	60.60 ₍₁₆₎	52.06 ₍₅₎	58.90 ₍₁₅₎	69.09 ₍₇₎	41.47 ₍₅₎	42.46 ₍₆₎	89.34 ₍₉₎	49.67 ₍₆₎	98.60 ₍₁₂₎	71.41 ₍₃₎	133 ₍₂₀₎	
	BA	20.87 ₍₁₀₎	32.54 ₍₇₎	50.33 ₍₆₎	41.09 ₍₉₎	57.27 ₍₅₎	34.10 ₍₅₎	34.01 ₍₃₎	69.10 ₍₇₎	33.97 ₍₃₎	45.58 ₍₇₎	33.35 ₍₅₎	32.23 ₍₉₎	
	Bw/Bt	32.20 ₍₄₎	21.73 ₍₆₎	48.66 ₍₆₎	30.13 ₍₈₎	32.72 ₍₅₎	32.25 ₍₆₎	21.24 ₍₃₎	21.24 ₍₃₎	63.52 ₍₈₎	30.29 ₍₈₎	38.14 ₍₉₎	21.01 ₍₂₎	
	Bck1	30.08 ₍₅₎	20.87 ₍₄₎	45.74 ₍₃₎	21.91 ₍₄₎	29.09 ₍₄₎	22.12 ₍₃₎	14.09 ₍₂₎	14.09 ₍₂₎	49.97 ₍₉₎	24.73 ₍₃₎	10.23 ₍₂₎	27.13 ₍₃₎	11.05 ₍₁₎
	Bck2	21.74 ₍₂₎	19.87 ₍₃₎	38.71 ₍₅₎	20.54 ₍₃₎	24.54 ₍₂₎	21.19 ₍₃₎	14.07 ₍₂₎	14.07 ₍₂₎	30.28 ₍₃₎	18.21 ₍₂₎	14.88 ₍₂₎	25.32 ₍₃₎	11.03 ₍₂₎
Clay (%)	Ap/A	18.14 ₍₄₎	20.9 ₍₃₎	20.42 ₍₃₎	22.1 ₍₄₎	23.3 ₍₃₎	30.6 ₍₃₎	13.29 ₍₃₎	23.0 ₍₂₎	20.4 ₍₂₎	28.2 ₍₃₎	26.1 ₍₂₎	25.3 ₍₃₎	
	BA	20.60 ₍₄₎	26.6 ₍₄₎	20.67 ₍₃₎	23.6 ₍₃₎	23.0 ₍₄₎	37.2 ₍₄₎	12.02 ₍₃₎	28.1 ₍₃₎	21.2 ₍₃₎	32.9 ₍₄₎	38.8 ₍₃₎	34.6 ₍₃₎	
	Bw/Bt	20.92 ₍₃₎	28.0 ₍₃₎	31.39 ₍₄₎	23.9 ₍₃₎	29.2 ₍₄₎	40.6 ₍₃₎	15.82 ₍₄₎	15.82 ₍₄₎	36.5 ₍₂₎	27.6 ₍₂₎	37.5 ₍₃₎	34.2 ₍₂₎	
	Bk	18.81 ₍₂₎	26.1 ₍₃₎	32.06 ₍₃₎	25.1 ₍₃₎	27.7 ₍₃₎	41.77 ₍₄₎	11.39 ₍₃₎	11.39 ₍₃₎	38.6 ₍₃₎	26.9 ₍₂₎	40.9 ₍₃₎	35.4 ₍₃₎	
	Bc	21.09 ₍₃₎	26.3 ₍₃₎	31.81 ₍₂₎	26.0 ₍₃₎	24.8 ₍₃₎	41.18 ₍₄₎	5.70 ₍₄₎	5.70 ₍₄₎	35.7 ₍₃₎	23.6 ₍₁₎	43.8 ₍₄₎	36.2 ₍₄₎	

Fig. 2 Distribution of total selenium contents in the soils at different weathering stages in each parent material



highest in the shale, followed by a statistically similar mean value ($n = 45$) in the loess parent material and significantly lower value in the alluvial and sandstone derived soils.

The hypothesis of depth levels \times parent material interaction was rejected ($F = 7.38$, $df = 12$, $p \geq 0.0001$), implying that the trend of distribution of metal oxide selenium as absolute concentration with depth varied with the parent materials. In the alluvium and sandstone soils, the change in oxide bound selenium with depth was statistically non-significant, and in loess and shale, the oxide bound selenium fraction increased towards the surface.

The highly weathered soils of loess and shale had a higher absolute concentration of metal oxides bound selenium than similar soils of sandstone and alluvium in several surface horizons. However, all the three development stages in alluvium and sandstone had similar metal oxides selenium concentration. The highly weathered soils in loess (Chakwal soil series) and shale (Murree soil series) had high selenium which increased towards the surface. The hypothesis of depth levels \times soil(pm) interaction effect was rejected ($F = 3.95$, $df = 32$, $p \geq 0.0001$), implying that the variation in oxide bound

selenium with depth changed with the weathering stage (Fig. 4). The difference in soils in metal oxide bound selenium at different weathering stages was mostly non-significant, except in the case of highly weathered soils of loess and shale. The Pearson coefficient correlation between metal oxide selenium was significant with oxalate extractable iron ($r = 0.58$; $p < 0.0001$) and non-significant with crystalline iron oxides suggesting a stronger association of the selenium fraction with the poorly crystalline iron.

Organic selenium

Soil selenium fraction extracted with hydrochloric acid, organic selenium, comprises of seleno-amino acids and organo-selenium derived from plant tissues or inorganic selenium and incorporated in organic fraction abiotically or by microbiological activity (Hagrova et al. 2005). The selenium fraction varied between 7 and 190 $\mu\text{g kg}^{-1}$ of soil, and loess-derived soils had the highest mean ($n = 45$) concentration followed by statistically lesser concentration values in alluvium and shale and a further lower mean value

Table 4 Mean soil selenium fractions averaged over the different soils in each parent material

	Horizon	Ca-Se	Oxides-Se	Organic-Se	Humic-Se	Sulfide-Se	Residual-Se	Total-Se
mg kg ⁻¹								
Alluvium	Ap/A	53 ₍₁₁₎	22 ₍₁₎	68 ₍₃₎	43 ₍₈₎	32 ₍₅₎	168 ₍₂₎	435 ₍₆₎
	BA	53 ₍₁₃₎	23 _(0.8)	71 ₍₃₎	37 ₍₆₎	33 ₍₅₎	168 ₍₂₎	451 ₍₅₎
	Bw/Bt	55 ₍₁₁₎	27 ₍₃₎	62 ₍₄₎	30 ₍₄₎	36 ₍₅₎	168 ₍₃₎	424 ₍₇₎
	Bt2/Btk1/C1	53 ₍₁₀₎	29 _(0.4)	60 ₍₃₎	32 ₍₅₎	38 ₍₄₎	171 ₍₁₎	418 ₍₁₎
	Bt3/Btk2/C2	52 ₍₁₂₎	36 ₍₄₎	66 ₍₄₎	28 ₍₄₎	38 ₍₆₎	172 ₍₂₎	429 ₍₂₎
Loess	Ap/A	57 ₍₇₎	54 ₍₇₎	137 ₍₃₅₎	51 ₍₄₎	77 ₍₉₎	150 ₍₁₉₎	537 ₍₅₈₎
	BA	82 ₍₈₎	50 ₍₇₎	133 ₍₂₁₎	49 ₍₅₎	85 ₍₇₎	144 ₍₁₈₎	551 ₍₃₈₎
	Bw/Bt	64 ₍₂₎	60 ₍₇₎	125 ₍₂₀₎	56 ₍₇₎	105 ₍₁₁₎	137 ₍₁₈₎	551 ₍₃₃₎
	Bk1/BC1	79 ₍₁₀₎	40 _(0.68)	111 ₍₁₀₎	49 ₍₃₎	105 ₍₈₎	135 ₍₁₆₎	530 ₍₂₁₎
	Bk2/BC2	53 ₍₅₎	35 ₍₅₎	121 ₍₁₈₎	38 ₍₄₎	96 ₍₁₃₎	132 ₍₁₂₎	483 ₍₄₀₎
Sandstone	Ap/A	41 ₍₄₎	31 ₍₂₎	16 ₍₂₎	18 ₍₂₎	27 ₍₁₎	171 ₍₄₎	312 ₍₁₀₎
	BA	38 ₍₁₎	22 ₍₂₎	18 ₍₄₎	21 ₍₂₎	36 ₍₄₎	163 _(0.4)	302 ₍₃₎
	Bw/Bt	35 ₍₁₎	20.83 _(1.83)	15 ₍₂₎	22 ₍₂₎	40 ₍₃₎	166 _(0.9)	308 ₍₂₎
	Bk1/Bck1	40 ₍₄₎	23.82 _(2.66)	19 ₍₄₎	12 _(0.5)	38 ₍₁₎	166 _(0.2)	195 ₍₁₁₎
	Bk2/Bck2	31 ₍₃₎	20.07 _(1.72)	14 ₍₃₎	15 ₍₂₎	32 ₍₂₎	146 ₍₁₁₎	265 ₍₂₃₎
Shale	Ap/A	76 ₍₁₀₎	61.41 _(27.92)	84 ₍₃₁₎	106 ₍₇₎	172 ₍₁₁₎	2072 ₍₁₀₂₎	2620 ₍₁₁₀₎
	BA	77 ₍₆₎	99.28 _(45.47)	87 ₍₃₀₎	129 ₍₂₁₎	196 ₍₁₂₎	1947 ₍₉₆₎	2573 ₍₁₀₆₎
	Bw/Bt	64 ₍₃₎	22.53 _(1.42)	24 ₍₂₎	94 ₍₇₎	211 ₍₁₃₎	282 ₍₃₎	758 ₍₁₃₎
	Bck1/BK	64 ₍₇₎	22.00 _(0.65)	24 ₍₂₎	98 ₍₁₁₎	207 ₍₁₁₎	283 ₍₂₎	740 ₍₁₆₎
	Bck/BC	64 ₍₃₎	24.69 _(1.25)	20 ₍₄₎	97 ₍₃₎	219 ₍₁₀₎	282 ₍₃₎	736 ₍₁₂₎

in the sandstone derived soils. The loess soils also had the highest organic selenium as a fraction of total selenium in these soils. Interestingly, the shale soils had the lowest organic selenium when expressed as a fraction of total selenium. As presented later, the shale soils had a large proportion of total selenium as bound with sulfide or as recalcitrant form.

The hypothesis of depth levels \times parent material interaction was rejected ($F = 4.4$, $df = 12$, $p \geq 0.0001$) implying that the mean of organic selenium, when averaged over the three soils in each parent material, had different distribution pattern with profile depth in at least one parent material. In the shale and loess derived soils, organic selenium increased towards the surface (Table 4). The significant test statistics resulted mainly from the higher organic selenium on the surface in shale-derived soils.

The organic selenium was significantly correlated with oxalate extractable iron (poorly crystalline iron oxides) in the soils, Pearson coefficient correlation 0.31 ($p < 0.0001$), and in non-significant correlation with TOC and clay. The absolute concentration of organically bound selenium was affected by weathering, especially in the case of loess and shale derived soils, while the sandstone-derived soils of various development stages differed non-significantly in terms of organic selenium contents. In alluvial soils,

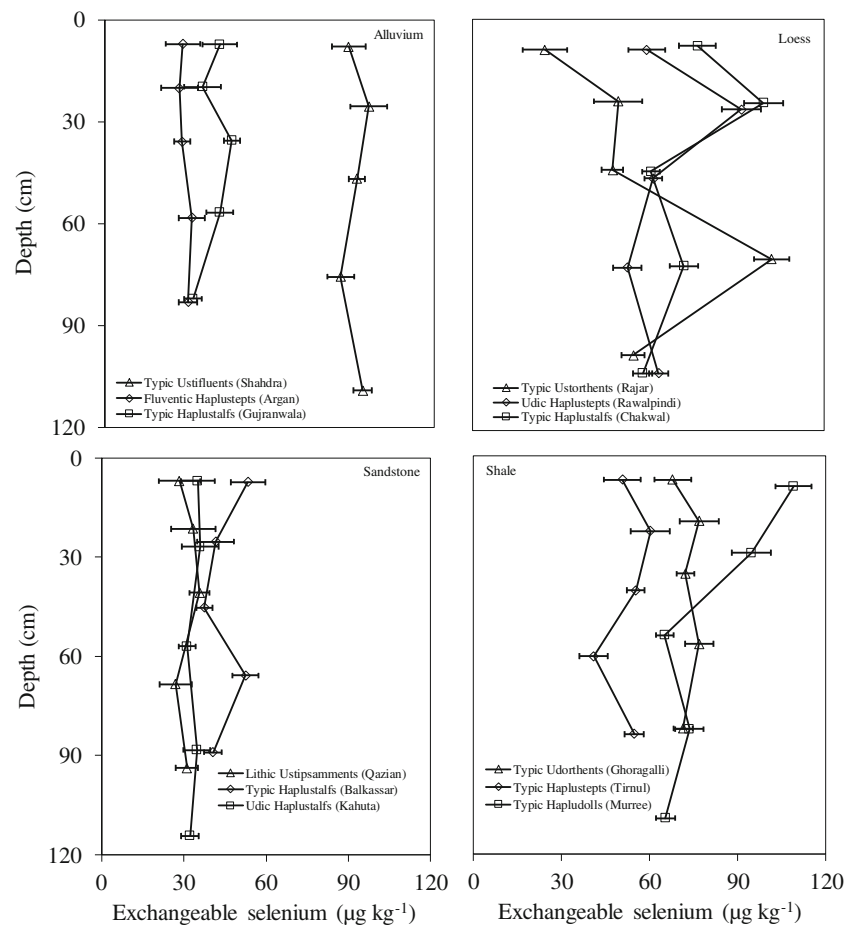
organic selenium remains unchanged with weathering as well. The hypothesis of depth levels \times soil (pm) interaction was rejected ($F = 3.56$, $df = 32$, $p \geq 0.0001$), implying that organic selenium contents changed differently with soil type in at least one parent material throughout the profile depth (Fig. 5).

Humic bound selenium

The selenium extracted with sodium hydroxide, humic bound selenium, varied between and 200 $\mu\text{g kg}^{-1}$ soil in the dataset. The shale-derived soils had the highest mean ($n = 45$) humic bound selenium contents, followed by a statistically lower value in each of the loess, alluvium, and sandstone parent materials. The humic bound selenium fraction followed the order of organic selenium and total organic carbon ($r = 0.28$, $p < 0.0001$). The humic bound selenium fraction was also correlated to crystalline iron oxides with the Pearson coefficient correlation of 0.65 ($p < 0.0001$). There was a lesser but significant relationship with the amorphous iron oxides ($r = 0.38$).

The hypothesis of depth levels \times parent material interaction was rejected ($F = 2.23$, $df = 12$, $p \geq 0.02$), implying that the mean of humic bound selenium, when averaged over the three-soil development stage, had a different pattern with

Fig. 3 Distribution of exchangeable selenium contents in soils at different weathering stages in each parent material



depth in at least one parent material. The significant statistics were related to probably shale having greater organic selenium at the surface. The humic bound selenium in sandstone was lowest throughout the profiles depth as indicated by the mean ($n = 15$) and was highest in shale (Table 4). The humic bound selenium concentration similarly followed the order of organic selenium and correlated with the iron oxides. As a fraction of total selenium, humic selenium was significantly high in the shale followed by loess, sandstone, and alluvium derived soils.

The hypothesis of depth levels \times soil(pm) interaction was rejected ($F = 1.83$, $df = 32$, $p \geq 0.018$), implying that the humic selenium concentration changed the profiles throughout the depth in accordance with the soil development in different parent materials. The difference in humic selenium concentration at various depths among the soils of three development stages in alluvium and sandstone was generally insignificant, while in loess and shale the differences were significant at several depths (Fig. 6). The concentration of humic bound selenium increased with weathering especially in the case of shale and loess derived soils and remained unchanged in sandstone and alluvium derived soils.

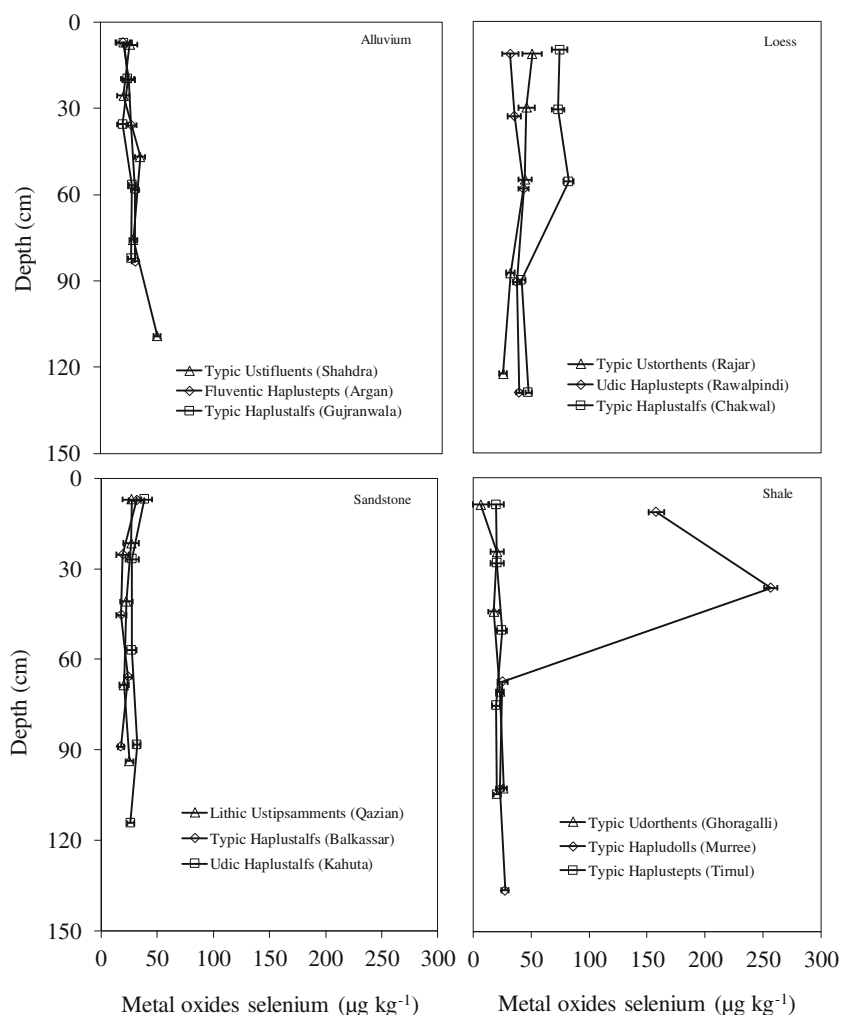
Sulphide bound selenium

The sulfide bound selenium concentration varied between 10 and $315 \mu\text{g kg}^{-1}$ and was 2.2 to 36.2% of total selenium in soils. The chemical treatment at step 5 (8 M HNO_3) dissolves various sulfide minerals (e.g., Pyrite) in which selenide is substituted for sulfide (Hagrova et al. 2005). Sulfide mineral bound selenium had a strong positive relation with crystalline iron oxides ($r = 0.71$).

A significant positive correlation of sulfide selenium with organic and humic bound selenium ($r = 0.70$) and clay content ($r = 0.58$) may be due to indirect relation as clay increases with weathering. As a percent of total selenium, sulfide bound selenium had little relation with Eh but stronger relation existed with crystalline iron oxides and clay. The shale-derived soils had the highest mean sulfide bound selenium followed by the significantly lower mean value in the loess and by a statistically similar mean ($n = 45$) values in alluvium and sandstone derived soils. As a percent fraction of total selenium, sulfide bound selenium was high in shale derived soils followed by those loess, sandstone, and alluvium.

The mean ($n = 15$) distribution of sulfide bound selenium concentration changed a little with the source of parent

Fig. 4 Distribution of metal oxide selenium contents in soils at different weathering stages in each parent material



material as the hypothesis of depth levels \times parent material interaction could not be rejected ($F = 0.98$, $df = 12$, $p \geq 0.48$), implying that the mean of the sulfide bound selenium had a similar pattern with depth (Table 4). The sulfide bound selenium was lesser in loess throughout the depth than shale and still greater than sandstone and alluvium. The sulfide bound selenium concentration distribution pattern with depth in different parent materials mimics very closely the crystalline iron oxides distribution pattern among the soil parameters and the humic bound selenium fraction among the selenium fractions.

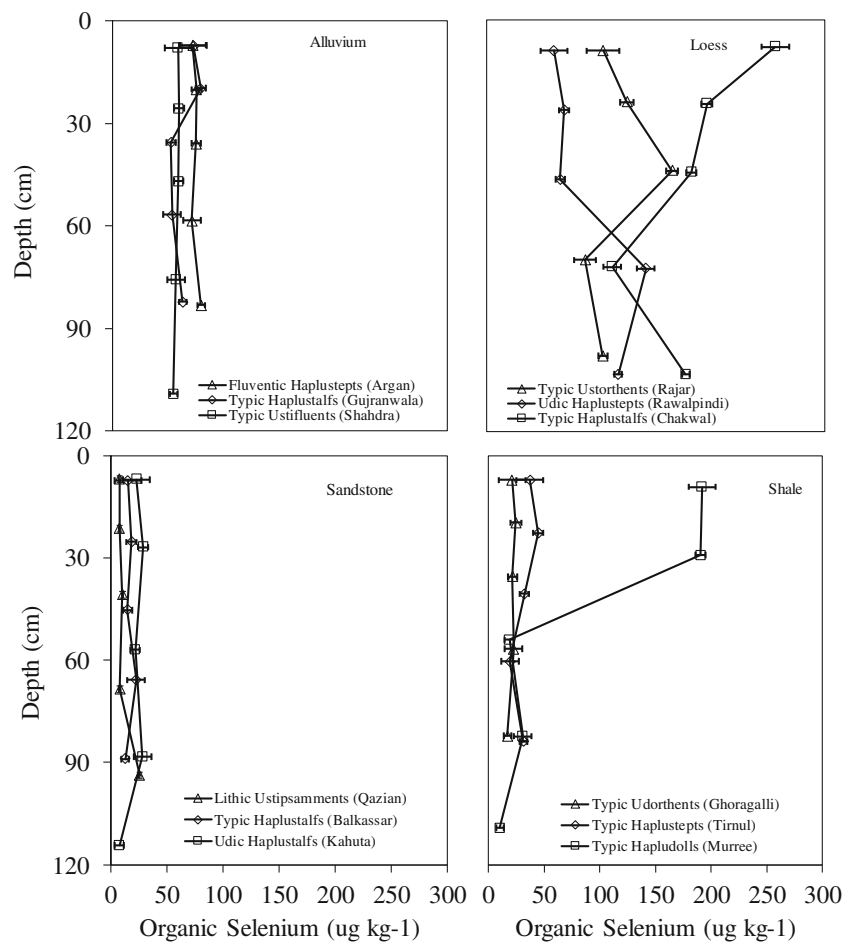
As a fraction of total selenium, sulfide bound selenium had a different pattern in the parent material profile than as absolute concentration. The surface of shale sulfide bound selenium as a fraction of total selenium was low at the surface of shale where selenium occurred dominantly as organic and humic selenium, owing to their occurrence under forest. The sulfide bound selenium decreased towards the surface in highly weathered soils of shale and loess and remained unchanged in alluvium and sandstone. The hypothesis of depth levels \times soil (pm) interaction could not

be rejected ($F = 1.01$, $df = 32$, $p \geq 0.46$), implying that sulfide bound selenium concentration (also as a fraction of total selenium) had a statistically similar pattern of distribution with depth in soils of different development stages of these parent materials (Fig. 7).

Residual selenium

The residual selenium varied between 16 and 6306 µg kg⁻¹ in the dataset and was 27 to 56% of total selenium. The last chemical treatment (HF and mixed acids solution) used to decompose the structure of the silicate in compounds of selenium minerals embedded or occluded in siliceous materials (Hagrova et al. 2005). The shale derived soils had the highest residual selenium, followed by lower but statistically similar mean ($n = 45$) values in loess, alluvium, and sandstone. The residual selenium was controlled by the total selenium as indicated by the Pearson coefficient correlation $r = 0.99$ ($p < 0.0001$). The hypothesis of depth levels \times parent material interaction could not be rejected ($F = 19.24$, $df = 12$, $p \geq 0.0001$), implying that the mean

Fig. 5 Distribution of mean organic selenium contents in soils at different weathering stages in each parent material



concentration of residual selenium had a different pattern when averaged over the soils in at least one parent material (Table 4). As a fraction of total selenium, the highest selenium was in the surface samples of the shale soils, whereas the sandstone-derived soils had the highest selenium throughout the depth followed by alluvium and sandstone.

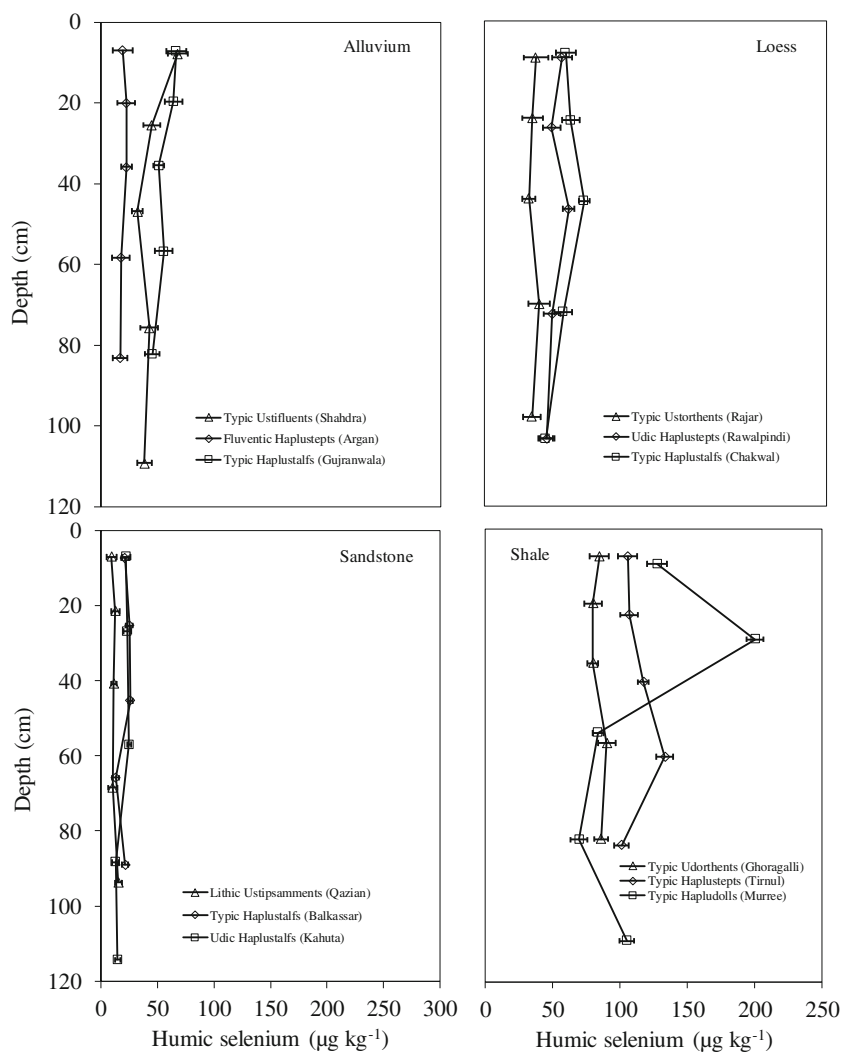
The shale-derived soil had higher selenium throughout the profile’s depth, while the highest residual selenium was in the surface horizons. The shale inherently contains more selenium minerals causing the residual selenium to increase in shale compared with the other parent materials. The sandstone had the highest residual selenium 56% as a fraction of total selenium followed by shale 45% and 26 to 39% selenium in alluvium. The residual selenium decreased in highly weathered soils of loess, whereas in the case of the alluvium and sandstone-derived soils, residual selenium remained unaffected with profile depth and in the shale surface of highly weathered soil had higher residual selenium. As a percent fraction of total selenium, residual selenium was more in the highly weathered soils of loess and shale, whereas in alluvium and sandstone, it remained

unchanged with depth due to weathering (Fig. 8). The hypothesis of depth levels × soil (pm) interaction effect was rejected ($F = 10.53, df = 32, p \geq 0.0001$), implying that with residual selenium contents changed differently with soil development stage in each parent material throughout the profile depth.

Discussion

The variations in total selenium contents are inherited from the source of different rocks (Yang et al. 2016). The greater selenium minerals in shale parent material contributed to the high total selenium in shale than sandstone, alluvium, and loess. As previous studies confirmed the high contents of total selenium of the shale may relate to lithology (Lopes et al. 2017). The sedimentary rocks are rich in selenium contents as compared with the igneous rocks (Armstrong et al. 2018). The granite and rhyolite are low selenium igneous rocks, whereas andesite and basalt are high in selenium contents; in other words, high siliceous rocks have low selenium contents than mafic rocks,

Fig. 6 Distribution of humic bound selenium contents in soils at different weathering stages in each parent material.

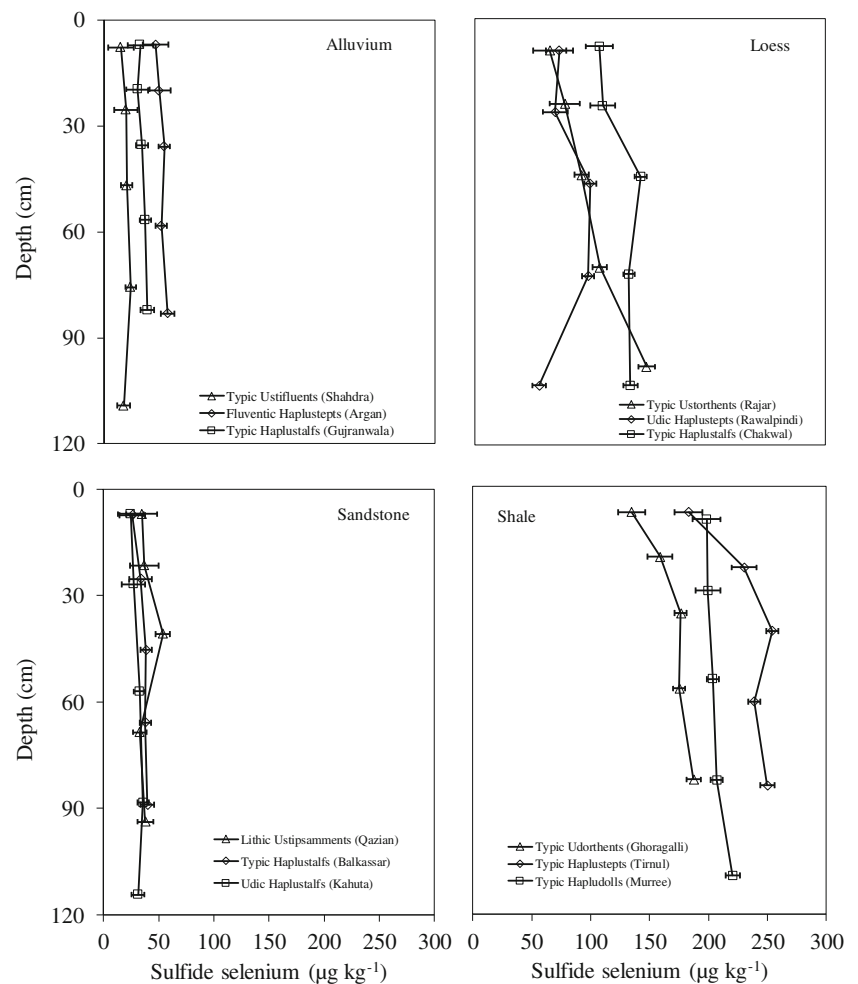


thus also explaining the mean low values of selenium in sandstone and alluvium, both consisting of large quartz. The distribution of total selenium along the profile depth changed uniquely in each parent material, depending on the soil genesis and weathering stage. The Hapludoll on shale caused the mean total selenium to increase several folds; similarly, the surface of the Ghoragalli soil series had very high organic carbon. The Murree and Ghoragalli soils occurred under coniferous forest in sub-humid to a humid climate and had the highest total organic carbon which leads to high mean selenium in the shale (Supriatin et al. 2016). Although less pronounced in the loess Alfisols, greater selenium at the surface of Chakwal soil series was observed and was associated with the accumulation of organic matter. Subsequently, we demonstrated that greater total selenium was due to greater organic selenium. The soil-forming factor vegetation is more dominant than the rainfall which led to the accumulation of organic selenium at the surface (Xiao et al. 2020). Pedogenesis in the alluvium and sandstone has caused little or no change in total

selenium within the soil profiles. The Haplustalfs and Ustifluents/Psamments had no significant difference throughout depth (Fig. 2).

The shale- and loess-derived soils had significantly greater mean water-soluble and exchangeable selenium concentration than the alluvial and sandstone soils. The sandstone-derived soils had the lowest water-soluble and exchangeable selenium concentration. As a fraction of total selenium, water-soluble and exchangeable selenium was lowest in the shale derived soils. The sandstone, alluvium, and loess derived soils had water-soluble and exchangeable selenium equally in a greater proportion of total selenium. Water-soluble and exchangeable selenium increased with advanced weathering due to increased exchange sites provided by argillaceous clay, oxides of iron, and organic compounds (Xing et al. 2015). The release of exchangeable and soluble selenium from these solid phases reflects their source to replenish the interstitial selenium. The sorption of selenium on organic matter and calcium carbonate is reported in the calcareous system (Smažiková et al. 2019; Lopes et al. 2017).

Fig. 7 Distribution of mean sulfide bound selenium contents in soils at different weathering stages in each parent material

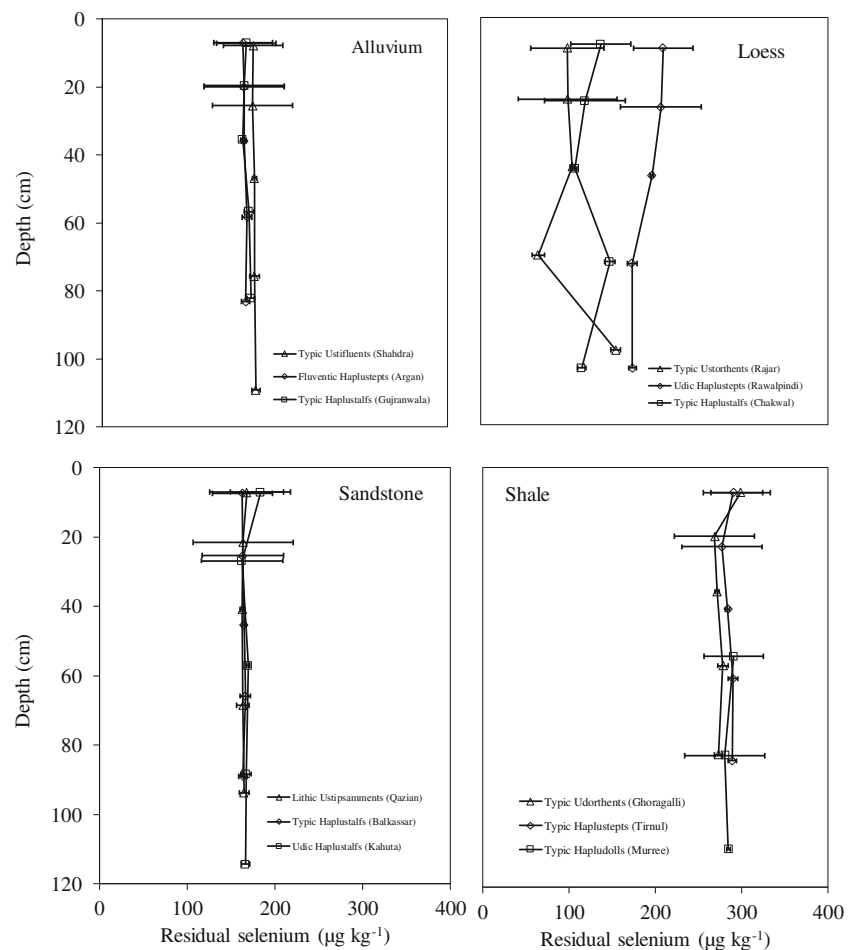


The highest metal oxide selenium may relate to high extractable iron and manganese oxides (Wang et al. 2015). As presented earlier, the shale and loess soils had high extractable iron. The weathered loess soil profiles also had a visible concentration of iron and manganese in the soil profiles. Selenium-enriched bedrock provided a material source for selenium in shale parent material, which inherently contains high selenium bearing minerals (Ren and Yang 2014). The poorly ordered oxides are sensitive to redox gradients and transform to crystalline oxides, resulting in high metal oxides selenium concentration (Kim et al. 2017; Wang et al. 2019). Iron and manganese oxide bound selenium accounts for most of the total selenium in high selenium soils derived from pyritic, black carbonaceous slate, and volcanic material (Bullock et al. 2018). Most of the selenium is adsorbed on clays and iron and manganese oxides (Bakather et al. 2017). Synthetic ferrihydrite, goethite, and lepidocrocite were compared for adsorption of selenate (Das et al. 2013) and reported ferrihydrite, having an order of magnitude higher in surface area than goethite, also leading to the higher adsorption capacity. The selenium removal from leachate reduces with the use of goethite and ferrihydrite. The organoselenium compounds are

adsorbed on poorly crystalline iron oxides (Donovan and Ziemkiewicz 2013). Because of the heterogeneity and complexity of the organic matter and adsorbent surfaces, the adsorption and desorption mechanisms of natural organic matter on mineral surfaces are not completely understood. Interaction through ligand exchange between iron oxides and natural organic matter surfaces through carboxyl and hydroxyl functional groups were proposed (Chi and Amy 2004). Organic selenium significantly correlated with dithionite extractable selenium; it may be noted that crystalline aluminum oxides may not exist in these soils of pH range 6.8 to 8.2 and the aluminum extracted with dithionite may have desorbed from organic matter.

The organic selenium could serve as plant available selenium either directly or indirectly by mineralization, and the soil selenium studies that do not include determination of organic selenium may be ignoring the important pool of soil selenium (Supriatin et al. 2016). The nature of the organic matter was reported to be important in weathering and distribution of selenium (Smažiková et al. 2019). It is interesting that the shale soils also had significantly greater humic bound selenium as that of the absolute concentration values, compared

Fig. 8 Residual selenium contents distribution in soils profiles at different weathering stages in each parent material.



with other soils parent materials. The values in the shale are like those reported by Kulp and pratt (2004). The Murree and Ghoragalli soils occurred under the coniferous forest in sub-humid to a humid climate and had the highest total organic carbon which led to higher mean selenium in the shale. The vegetation type is more important than the effect of precipitation on organic selenium accumulation (Li et al. 2017).

The humic compounds are the end products of the decomposition of soil organic matter. Sodium hydroxide (0.5 M) extracts both fulvic acid and humic acid in which selenium occurred in the form of selenoamino acids in the proteins or peptides. Humic acid selenium fraction expressed as a mass ratio to total selenium also had a strong significant correlation with crystalline iron oxides ($r = 0.38$), indicating a correlation between adsorbate and adsorbing surface as fulvic acid adsorbs on goethite surfaces over a wide range of pH (Bakather et al. 2017). The organic and humic compounds containing selenium are formed first by the release and uptake during oxidative weathering of minerals, and the decomposition of organic matter transforming to humus compounds containing selenium which are resistant to further weathering (Qin et al. 2013). During weathering and formation of soils, there is

often an increase in selenium in some cases decay of accumulator plants, building up high selenium concentration on the surface soils. Although there is a stronger correlation with crystalline iron oxides, as well as a significant positive relationship with the total organic carbon, implying that humus selenium increases as the total organic carbon increases. Selenate forms outer-sphere complexes with the amorphous and crystalline hydroxides of iron (Imran et al. 2015) and on hematite selenate directly interact with iron by inner-sphere complexes.

The shale derived soils are rich pyrite where selenium substitutes for sulfur (Matamoros-Veloza et al. 2011). Selenium in soils is related to the occurrence of sulfide minerals and the sedimentary rocks contain more selenium than the igneous rocks in most cases. The sulfide selenium minerals are oxidized by microorganisms and decreased the sulfide bound selenium as the oxidation of pyrite transformed the sulfide bound selenium to oxidized selenium forms (Xiao et al. 2020). Since the soils are at a relatively early stage of development, the effect of parent materials is strong. The high contents of residual selenium in the shale may relate to lithology (Parnell et al. 2016). The residual selenium is the largest selenium fraction accounting for $\geq 80\%$ of the total selenium.

Conclusion

Lithology controlled the total selenium contents, and within a parent material pedogenesis, had affected the distribution of selenium forms. The total selenium and the selenium bound with humic compounds, sulfide bound, and the recalcitrant were greater in the shale soils followed by those developed in the loess, alluvium, and sandstone. The ion-exchangeable, metal oxides bound, and organic matter bound selenium were more in loess or equal with that of shale. Organic and humic bound selenium increased with weathering especially in case of loess and shale. The sulfide bound selenium was higher in the least weathered shale soils and related to redox conditions, highly correlated with humic compound selenium. The recalcitrant and total selenium remained unchanged with weathering in all parent materials except loess. Evaluation of the selenium forms and species enabled us to estimate the occurrence of selenium deficiency and toxicity in soils derived from various parent materials. We recommend further study of the selenium ionic species and bioavailability in soils derived from various parent materials.

Appendix

Table 5 Mean Cation exchange capacity of soils across parent materials

Parent material	Horizon	Average depth (cm)	CEC (cmol _c /kg)
Alluvium	Ap/A	9	23.54 _(1.14)
	BA	29	23.00 _(0.98)
	Bw/Bt	48.5	22.79 _(1.17)
	Bt2/Btk1/C1	67	20.69 _(0.59)
	Bt3/Btk2/C2	91	18.19 _(1.02)
Loess	Ap/A	9	32.67 _(0.75)
	BA	24	29.72 _(0.86)
	Bw/Bt	44	30.96 _(1.30)
	Bk1/BC1	70	28.02 _(1.03)
	Bk2/BC2	98	26.44 _(1.01)
Sandstone	Ap/A	7.5	17.11 _(0.53)
	BA	22.5	15.59 _(0.67)
	Bw/Bt	45	16.31 _(0.59)
	Bk1/Bck1	74.5	14.97 _(0.42)
	Bk2/Bck2	99	14.50 _(0.61)
Shale	Ap/A	10	40.33 _(0.42)
	BA	35	37.87 _(0.28)
	Bw/Bt	60	36.90 _(0.33)
	Bck1/BK	82	36.62 _(0.31)
	Bck/BC	102	36.01 _(0.43)

References

- Amin R, Ikram M (2007) Keys to soils of punjab and sindh. Ministry of Food Agriculture and Livestock, Government of Pakistan. 121 pp
- Armstrong JA, Parnell J, Bullock LA, Perez M, Boyce AJ, Feldmann J (2018) Tellurium, selenium and cobalt enrichment in Neoproterozoic black shales, Gwna Group, UK: deep marine trace element enrichment during the Second Great Oxygenation Event. *Terra Nova* 30:244–253. <https://doi.org/10.1111/ter.12331>
- Bakather OY, Kayvani FA, Khraisheh M, Nasser MS, Atieh MA (2017) Enhanced adsorption of selenium ions from aqueous solution using iron oxide impregnated carbon nanotubes. *Bioinorg Chem Appl* 2017:4323619–4323612. <https://doi.org/10.1155/2017/4323619>
- Bullock LA, Parnell J, Perez M, Armstrong JG, Feldmann J, Boyce AJ (2018) High selenium in the Carboniferous coal measures of Northumberland, North East England. *Int J Coal Geol* 195:61–74. <https://doi.org/10.1016/j.coal.2018.05.007>
- Chi FH, Amy GL (2004) Kinetic study on the sorption of dissolved natural organic matter onto different aquifer materials: the effect of hydrophobicity and functional groups. *J Colloid Interface Sci* 274(2004):380–391. <https://doi.org/10.1016/j.jcis.2003.12.049>
- Das S, Hendry MJ, Essilfie-Dughan J (2013) Adsorption of selenate onto ferrihydrite, goethite, and lepidocrocite under neutral pH conditions. *Appl Geochem* 28:185–193. <https://doi.org/10.1016/j.apgeochem.2012.10.026>
- Donovan JJ, Ziemkiewicz PF (2013) Selenium adsorption onto iron oxide layers beneath coal-mine overburden spoil. *J Environ Qual* 42:1402–1411. <https://doi.org/10.2134/jeq2012.0500>
- Fan J, Zeng Y, Sun J (2018) The transformation and migration of selenium in soil under different Eh conditions. *J Soils Sediments* 18:2935–2947. <https://doi.org/10.1007/s11368-018-1980-9>
- Hagrova I, Zembryoua M, Bajcan D (2005) Sequential and single step extraction procedure used for fractionation of selenium in soil samples. *Chem Pap* 59:93–98
- Imran M, Akhtar MS, Hassan S, Khan KS, Khalid A, Mehmood A, Rukh S (2015) Distribution of selenite and selenate with weathering in various parent materials. *Asian J Chem* 27:4417–4424. <https://doi.org/10.14233/ajchem.2015.19152>
- Imran M, Akhtar MS, Khan KS, Khalid A, Mehmood A, Rukh S, Nazeer G, Manzoor R (2016) Total and extractable soil selenium contents variation within and across the parent materials. *Int Network Nat Sci* 9:175–186
- Jackson ML, Lim CH, Zelazny LW (1986) Oxides, hydroxides and aluminosilicates. In: Klute A (ed) *Methods of soil analysis*. Part 1, vol 9. Agronomy Society of America, Madison 101 pp
- Kim YJ, Yuan K, Ellis BR, Becker U (2017) Redox reactions of selenium as catalyzed by magnetite: lessons learned from using electrochemistry and spectroscopic methods. *Geochim Cosmochim Acta* 199:304–323. <https://doi.org/10.1016/j.gca.2016.10.039>
- Kulp TR, Pratt LM (2004) Speciation and weathering of selenium in upper cretaceous chalk and shale from South Dakota and Wyoming, USA. *Geochim Cosmochim Acta* 68:3687–3701. <https://doi.org/10.1016/j.gca.2004.03.008>
- Kurokawa S, Berry MJ (2013) Selenium. Role of the essential metalloids in health. *Metal Ions Life Sci* 13:499–534. https://doi.org/10.1007/978-94-007-7500-8_16
- Li Z, Liang D, Peng Q, Cui Z, Huang J, Lin Z (2017) Interaction between selenium and soil organic matter and its impact on soil selenium bioavailability: a review. *Geoderma*. 295:69–79. <https://doi.org/10.1016/j.geoderma.2017.02.019>
- Loeppert RH, Hallmark CT, Koshy MM (1984) Routine procedure for rapid determination of soil carbonates. *Soil Sci Soc Am J* 48:1030–1033
- Lopes G, Avila FW, Guilherme LRG (2017) Selenium behavior in the soil environment and its implication for human health. *Cienc*

- Agrotecnol 41(6):605–615. <https://doi.org/10.1590/1413-70542017416000517>
- Matamoros-Veloz A, Newton RJ, Benning LG (2011) What controls selenium release during shale weathering? *Appl Geochem* 26:222–226. <https://doi.org/10.1016/j.apgeochem.2011.03.109>
- Mayorga IC, Astilleros JM, Fernández-Díaz L (2019) Precipitation of CaCO₃ polymorphs from aqueous solutions: the role of pH and sulphate groups. *Minerals* 9(3):178
- McLean EO (1982) Soil pH and lime requirement. In: Page AL (ed) *Methods of soil analysis. Part II, Chemical and microbiological properties*. American Society of Agronomy, Madison, pp 199–244
- Mehmood A, Akhtar MS, Imran M, Rukh S (2018) Soil apatite loss rate across different parent materials. *Geoderma*. 310:218–229. <https://doi.org/10.1016/j.geoderma.2017.09.036>
- Mehra OP, Jackson ML (1960) Iron oxide removal from soil and clays by dithionite-citrate buffered with sodium bicarbonate. *Clay Miner* 7: 317–327
- Natasha MS, Niazi NK, Khalid S, Murtaza B, Bibi I, Rashid MI (2018) A critical review of selenium biogeochemical behavior in soil-plant system with an inference to human health. *Environ Pollut* 234: 915–934
- Nelson DW, Sommers LE (1982) Organic matter. In: Page AL, Miller RH, Keeney DR (eds) *Methods of soil analysis. Part II, Chemical and microbiological properties*. American Society of Agronomy, Madison, pp 574–577
- Parnell J, Brolly C, Spinks S, Bowden S (2016) Selenium enrichment in Carboniferous Shales, Britain and Ireland: problem or opportunity for shale gas extraction? *Appl Geochem* 66:82–87
- Parnell J, Bullock L, Armstrong J, Perez M (2018) Liberation of selenium from alteration of the Bowland shale formation: evidence from the mam tor landslide. *Q J Eng Geol Hydrogeol* 51:503–508. <https://doi.org/10.1144/qjegh2018-026>
- Qin HB, Zhu JM, Liang L, Wang MS, Su H (2013) The bioavailability of selenium and risk assessment for human selenium poisoning in high-Se areas, China. *Environ Int* 52:66–74. <https://doi.org/10.1016/j.envint.2012.12.003>
- Ren H, Yang R (2014) Distribution and controlling factors of selenium in weathered soil in Kaiyang county, southwest China. *Chin J Geochem* 33:300–309. <https://doi.org/10.1007/s11631-014-0691-1>
- Santos AC, Pereira MG, Anjos LHC, Bemini TA, Cooper M (2016) Genesis of soils formed from mafic igneous rock in the Atlantic Forest environment. *Rev Bras Ci Solo* 40:e0150056. <https://doi.org/10.1590/18069657rbc20150056>
- SAS Institute Inc (2002) SAS/STAT software version 9.4 system for Windows,
- Smažiková P, Praus L, Száková J, Tremlová J, Hanč A, Tlustoš P (2019) The effect of organic matter rich amendments on selenium mobility in soil. *Pedosphere* 29(6):740–751. [https://doi.org/10.1016/S1002-0160\(17\)60444-2](https://doi.org/10.1016/S1002-0160(17)60444-2)
- Supriatin S, Weng L, Comans RNJ (2016) Selenium-rich dissolved organic matter determines selenium uptake in wheat grown on low-selenium arable land soils. *Plant Soil*:1–22. <https://doi.org/10.1007/s11104-016-2900-7>
- Walkley A (1947) A critical examination of a rapid method for determining soil organic carbon in soils: Effect of variations in digestion conditions and inorganic soil constituents. *J Soil Sci* 63:251–263. <https://doi.org/10.14202/vetworld.2013.963-967>
- Wang TH, Chiang CL, Wang CF (2015) The correlation between selenium adsorption and the mineral and chemical composition of Taiwan local granite samples. KIT Scientific Publishing, Germany
- Wang MK, Cui ZW, Xue MY, Peng Q, Zhou F, Wang D, Dinh QT, Liu YX, Liang DL (2019) Assessing the uptake of selenium from naturally enriched soils by maize (*Zea mays* L.) using diffusive gradients in thin-films technique (DGT) and traditional extractions. *Sci Total Environ* 689:1–9. <https://doi.org/10.1016/j.scitotenv.2019.06.346>
- Xiao K, Lu L, Tang J, Chen H, Li D, Liu Y (2020) Parent material modulates land use effects on soil selenium bioavailability in a selenium-enriched region of southwest China. *Geoderma* 376: 114554. <https://doi.org/10.1016/j.geoderma.2020.114554>
- Xing K, Zhou S, Wu X, Zhu Y, Kong J, Shao T, Tao X (2015) Concentrations and characteristics of selenium in soil samples from Dashan Region, a selenium-enriched area in China *Soil Sci. Plant Nutr* 61:889–897. <https://doi.org/10.1080/00380768.2015.1075363>
- Yang Q, Hou QY, Gu QB et al (2016) Study of geochemical characteristics and influencing factors of soil selenium in the typical soil profiles in Wuming County of Guangxi[J]. *Geoscience* 30(2):455–462
- Yattoo MI, Saxena A, Deepa PM, Habeab BP, Devi S, Jatav RS, Dimri U (2013) Role of Trace elements in animals: a review. *Vet World* 6(12):963–967